

Cosmic Ray in the Northern Hemisphere: Results from the Telescope Array Experiment

C. C. H. Jui[†], for the Telescope Array Collaboration

[†]*Department of Physics and Astronomy, University of Utah, Salt Lake City, UT, USA*

The Telescope Array (TA) is the largest ultrahigh energy (UHE) cosmic ray observatory in the northern hemisphere. TA is a hybrid experiment with a unique combination of fluorescence detectors and a stand-alone surface array of scintillation counters. We will present the spectrum measured by the surface array alone, along with those measured by the fluorescence detectors in monocular, hybrid, and stereo mode. The composition results from stereo TA data will be discussed. Our report will also include results from the search for correlations between the pointing directions of cosmic rays, seen by the TA surface array, with active galactic nuclei.

I. INTRODUCTION

The Telescope Array (TA) experiment [1] is a collaboration of 26 universities and research institutions in Japan, U.S., South Korea, Russia, and Belgium. The core of the collaboration consists of key members from the Akeno Giant Air Shower Array (AGASA) [2] in Japan, and the High Resolution Fly's Eye (HiRes) experiment [3]. TA combines the large area scintillation ground array technique developed by AGASA with that of the air fluorescence method pioneered by the Fly's Eye (FE) [4] at the University of Utah, and later improved by the HiRes group.

Telescope Array is located in the central western desert of Utah, near the city of Delta, about 250 km south west of Salt Lake City. The arrangement of the experiment is shown in figure 1. The new experiment consists of three fluorescence detector (FD) stations, marked in the figure by the green squares, located at the periphery of a ground array of 507 surface detectors (SD). Each SD unit, shown in figure 1 by the black squares, consists of a scintillation counter mounted on a raised steel frame. They are deployed in a square grid of 1.2 km nearest-neighbor spacing, and the full array covers a total of about 730 km².

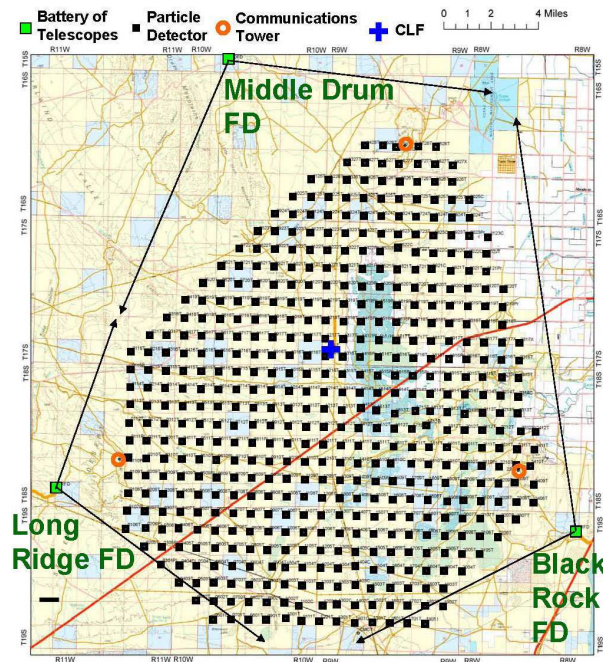


FIG. 1: The layout of the Telescope Array experiment. The black squares show the location of the 507 SD's. The green squares mark the FD stations at the periphery of the ground array. The three communications towers near the FD stations are indicated by orange circles. The central laser facility, at the center of the array, is shown by the blue cross.

Each of the three FD stations has a field of view (FOV) of about 30° in elevation and about 110° in azimuth. The central laser facility (CLF), which initially operated one vertical pulsed YAG laser (355 nm), is marked by

arXiv:1110.0133v1 [astro-ph.IM] 1 Oct 2011

the blue cross in figure 1. The location of the CLF is equidistant from all three FD stations so that the vertical pulses can be used for cross-calibration of the three stations independent of the aerosol concentration in the air. The three FD stations are also oriented such that the CLF lies at the center of view of each.

II. TA SURFACE DETECTORS

Each TA scintillation counter contains two slabs of double-layered plastic scintillators with an overall collection area of 3.0 m². The scintillation photons are collected by wavelength-shifting optical fibers laid in extruded grooves on the surface of the scintillators. All of the light collected from the top and bottom layers are each separately collected into a single photomultiplier tube (PMT). Each SD unit is powered entirely by its own solar panel-battery power supply, and communicates over a 24 GHz wireless point-to-point link with one of three communication towers. The towers are located near each of the three FD stations.

The SD counters are self-calibrated using minimum-ionizing cosmic muons. These muons provide a convenient unit of "vertical equivalent muon" (VEM). The output of the PMT from each scintillator is monitored continuously at 40 million samples per second (40 MSPS). Pulse data are recorded into a storage buffer when a cluster of at least 1/3 VEM is observed. An event trigger is formed when a minimum of three adjacent counters each detects a cluster of at least 3 VEM each. A typical event is shown in figure 2.

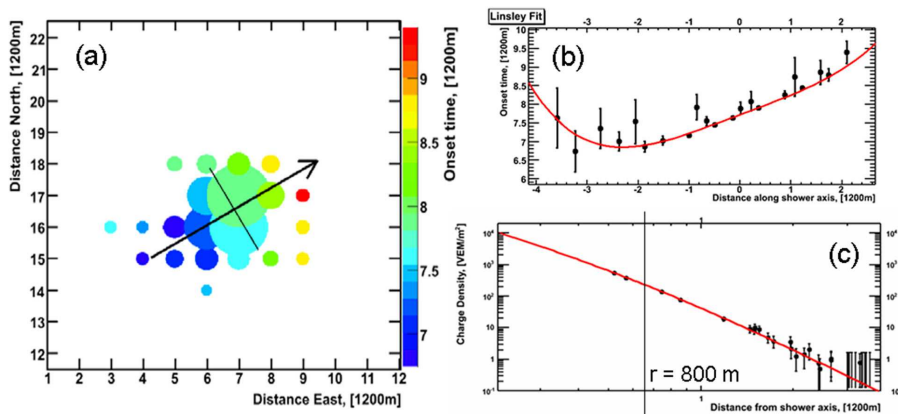


FIG. 2: (a) Left: Display of a typical air shower event captured by the TA surface detector array, where each circle represents a triggered SD unit. (b) Top Right: Fit of onset times of the triggered SD units to determine the shower arrival direction. (c) Bottom Right: Fit of the measured particle density vs. distance from the shower axis and the interpolation to obtain the density at 800 m (S800).

In figure 2(a), the hit counters and their recorded densities are shown by the circles and their area. The locations of the counters are given by row and column number (at 1.2 km spacing). The color scheme shows the arrival time in terms of equivalent distance traveled by light, divided by the detector spacing. The location, signal size, and onset time detected by each counter is used to fit for the core (centroid) location and arrival direction of the shower. This geometry fit uses a modified Linsley time delay function [5] to describe the curvature of shower front, and the AGASA lateral density function (LDF) [6] to predict the fall of density from the core of the shower. The result of this fit is illustrated in figure 2(b), which plots the onset time vs. distance along the direction indicated by the arrow in figure 2(a). The particle densities from the hit SD units are then plotted as a function of its perpendicular distance to the shower core, and the density at 800 meters (S800) is interpolated from the fit to the AGASA LDF function, as shown in figure 2(c). The S800 value is then compared to the average from simulated events (shown in figure 3) and the measured energy is interpolated according to the measured zenith angle.

III. TA FLUORESCENCE DETECTORS

A total of 38 fluorescence telescopes are divided into three stations. The first of these was constructed on Black Rock (BR) Mesa, at the southeastern corner of the surface array. A second station is located at Long Ridge (LR) on the southwestern flank of the SD array. The BR and LR detectors were built in Japan based

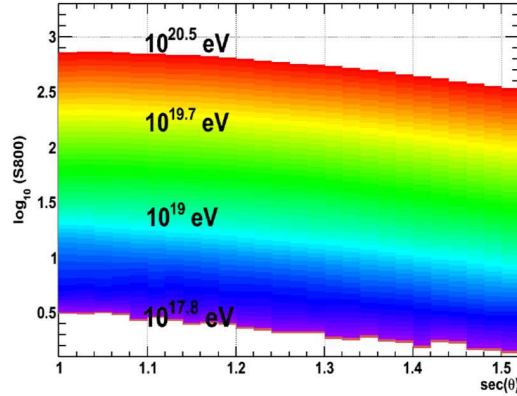


FIG. 3: The variation of the average particle density at 800 meters from core (S800) with the energy and zenith angle of simulated air showers. Energies of real air showers are determined by comparing the measured S800 to this plot.

on essentially the same specifications as the telescopes used by the HiRes experiment, but with larger mirrors of 6.8 m^2 area (compared to 5.2 m^2 for HiRes). Each site consists of 12 telescopes with 256-pixel (16×16 in a triangular lattice) cameras. Each pixel, instrumented by a hexagonal PMT, covers a cone of 1.1° in the sky. A typical event captured by the FD station at Black Rock is shown in figure 4. For each triggered event, the 10 MHz FADC data from each channel are scanned for pulses. Those channels containing a three sigma excess over background (primarily night sky) fluctuations are displayed as circles, with the area of the circle being proportional to the integrated pulse area.

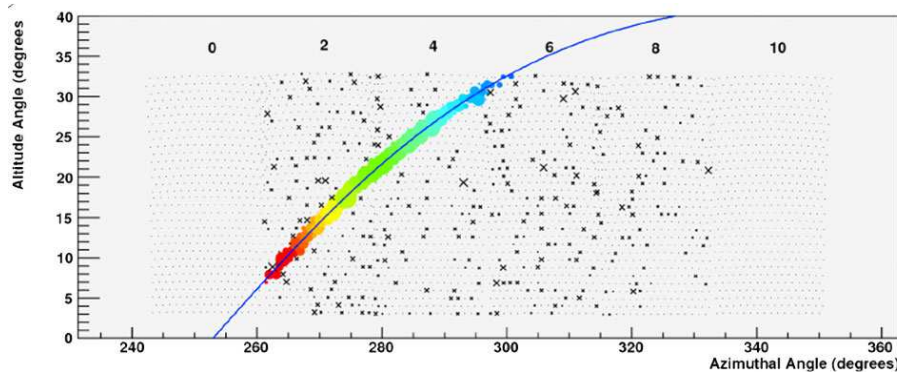


FIG. 4: Display of a typical downward air shower event captured by the FD station at Black Rock. The circles correspond to channels with pulses in excess of three sigma over the (night sky) background, and the area of the circles represent the integrated pulse area. Those pixels associated with the air shower are easily identified by their size and correlation in direction and time. The shower-detector plane (SDP) is shown by the fitted curve. The colors indicate arrival time of the signal light, with blue indicating the earliest and red the latest pulses.

As can be seen in figure 4, the pixels corresponding to the actual air shower are easily identified by their size as well as spatial and temporal correlation, and are marked in color. The pointing directions of these channels are then used to fit for a shower-detector plane (SDP). Because of the distortion inherent in the Miller cylindrical projection used for the event display, the fitted SDP appears as a curve in figure 4. The colors of event pixels indicate time progression: blue represents the earliest arrival times at the top of the event, and red represents the latest at the bottom. The event depicted was clearly a downward going air shower. Once the SDP is obtained, the trajectory of the air shower can be completely determined in one of two ways. For monocular observation, where only the measurement from a single fluorescence station is used, the shower axis can be determined by fitting the arrival time at each pixel to equation 1.

$$t_i = t_0 + \frac{R_P}{c} \tan \left(\frac{\pi - \psi - \chi_i}{2} \right) \quad (1)$$

As illustrated in figure 5(a), R_P is the impact parameter of the shower (nearest distance of approach of the

shower axis to the FD), and ψ is the angle made by the shower axis to the line of intersection between the SDP and the ground. The value t_0 physically corresponds to the time at which the shower passes the point of nearest approach. The output parameters from the timing fit are t_0 , R_P , and ψ . The inputs are the measured times t_i and the angles χ_i of the pixels involved in the event. As seen in figure 5(a), χ is the angle made between the PMT pointing direction (projected onto the SDP), and the ground, measured within the shower detector plane. Alternately, with two FD stations viewing the same event in stereoscopic mode, the shower trajectory can be determined from the intersection of the two SDPs. This stereo reconstruction method is illustrated in figure 5(b). Typically at energies in the ultra high energy (UHE) regime, monocular reconstruction gives R_P and ψ resolutions of about 10% and 5%, respectively, whereas the stereo reconstruction improves these to about 5% and 1°.

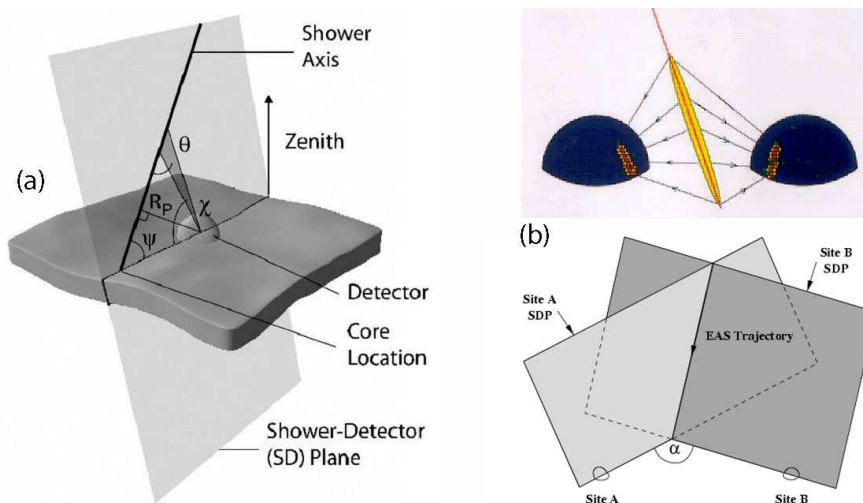


FIG. 5: (a) Illustration of the monocular FD time fit to determine the shower trajectory. (b) Illustration of the intersecting plane method of finding the shower axis for stereo FD observations.

Figure 6(a) shows the timing fit described above for the event shown in figure 4. The amount of curvature in the data determines the in-plane angle, ψ . For a given ψ , the overall slope of the data then determines the impact parameter, R_P . Having determined the shower trajectory, the pointing directions of the PMTs are then converted to slant depth. The signal is then fitted to a parametric function, usually the Gaisser-Hillas form [7] for the shower size vs. depth, and includes scattered and direct Čerenkov light in addition to the fluorescence signal. The profile fit for this same event is shown in figure 6(b). The Energy is extracted from the overall area of the curve, and the depth of the shower maximum, X_{max} , is extracted from the fit. Over many showers, the X_{max} values give a statistical measure of the composition of the primary particles.

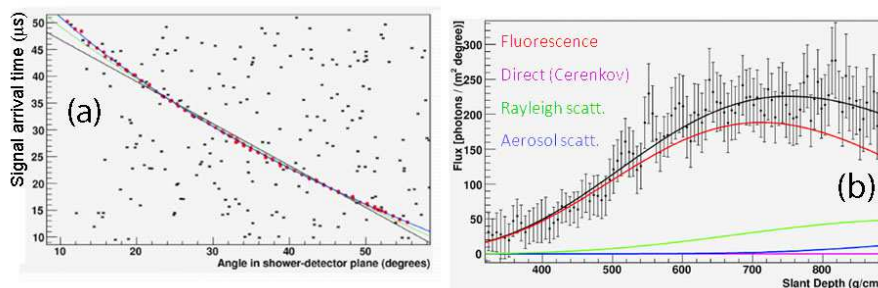


FIG. 6: (a) Timing fit to determine R_P and ψ . (b) Profile fit to determine the energy and X_{max} for the shower shown originally in figure 4.

The High Resolution Fly's Eye experiment used two alternative monocular reconstruction techniques. Between 1992-1996, the HiRes prototype, in the tower configuration (14 telescopes viewing up to 70° in elevation), operated in coincidence with the CASA/MIA arrays. The HiRes/MIA monocular reconstruction included the timing information from the MIA array. This combination became known as the hybrid reconstruction method,

and yields R_P and ψ resolutions comparable to that of stereo reconstruction. The Telescope Array experiment is primarily designed for hybrid FD reconstruction. An example of the hybrid timing fit for a TA event is shown in figure 7.

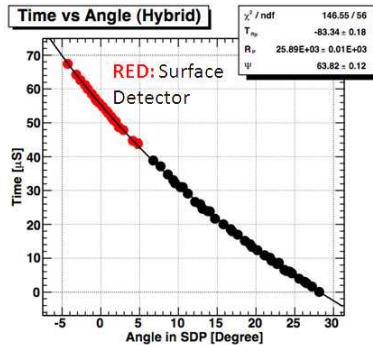


FIG. 7: Timing fit for a hybrid event that includes times of the surface detectors.

Previously for the HiRes-1 site, where the telescopes only view up to 17° , the observed tracks from air showers are too short for the timing fit alone to give reliable results. Instead, another variant of the monocular reconstruction was used that combined the timing and profile fits of figure 6. This technique uses the form of the shower profile to constrain the range of geometries. The profile-constrained fit (PCF) gives resolutions that are comparable to monocular fit at the highest energies for the one-layer HiRes-1 detector but quickly degrades and becomes unusable below about 3×10^{18} eV. The third fluorescence detector station on Middle Drum (MD) Mountain, located at the northern end of TA, was built with 14 refurbished telescopes from HiRes-1. This commonality between HiRes and TA allows us to compare the results of the two experiments directly. For this purpose, the initial analysis of the MD monocular FD data used exactly the same simulation and reconstruction codes as was used for HiRes-1, changing only the pointing geometry of the detectors, and lowering the trigger threshold in the simulation to reflect the reduced ambient background light.

IV. TA ENERGY SPECTRUM MEASUREMENT

One of the early objectives for building the Telescope Array experiment was to resolve the discrepancy between the observation of the Greisen-Zatsepin-K'uzmin [8] cut-off in the UHE cosmic ray spectrum. Using the fluorescence technique alone, HiRes reported the first observation of the GZK cut-off in 2008 [9], whereas earlier measurements by AGASA, using a scintillation ground array alone reported a continuing spectrum [10]. Figure 8 shows the monocular spectrum from the Middle Drum FD station from its first three years of observation. The HiRes monocular spectrum [9] is also shown in the figure. The MD station uses 14 refurbished telescopes from HiRes-1, the latter having provided most of the statistical significance for the GZK cut-off. The two sets of spectra are in excellent agreement both in the shape and overall normalization. The new TA result is also consistent with a flux suppression at the expected GZK threshold.

From a compilation of TA hybrid events seen by both the SD and the FD, the SD was seen to give a consistently higher energy. After the first year of observation, the SD energies was determined to be consistently 1.27 times higher than the FD energies. Figure 9(a) shows a histogram of the difference between the FD and SD energies, with the SD energies scaled down by 1.27. A scatter-plot of log FD energy vs log SD energy for the same events is shown in figure 9(b). The latter shows a linear relationship between the two energy measurements over the 1.5 decades of energy above 3×10^{18} eV.

Figure 10(a) shows the energy spectrum of UHE cosmic rays compiled from the first three years of TA surface array data. The energy of each event was rescaled by the factor of 1.27. This spectrum is overlaid with the monocular FD spectrum (previously shown in 8). With the rescaling of energies alone, the SD spectrum obtained is in excellent agreement with the monocular FD spectrum, and in turn, with the HiRes spectrum both in normalization and in shape. Figure 10(b) shows a preliminary hybrid spectrum from the Middle Drum FD data overlaid with the SD spectrum. Again the two are in excellent agreement. We have divided the three TA spectra shown (MD FD monocular, SD, and MD FD hybrid) and the HiRes spectrum into three plots in order to avoid clutter. The conclusion we draw here is that with a 1.27 energy scaling factor for the SD, the TA SD and MD FD spectra are completely consistent with the HiRes results. Monocular and hybrid spectra

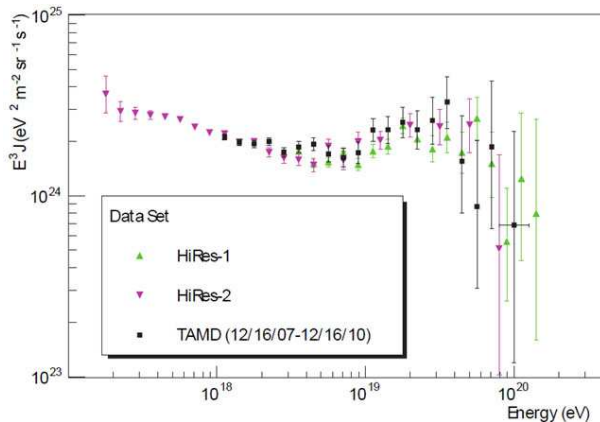


FIG. 8: TA monocular spectrum from the Middle Drum FD station from its first three years of observation, overlaid with the monocular spectra from HiRes. The TA and HiRes spectra are in excellent agreement. The TA spectrum is also consistent with the presence of the GZK cut-off.

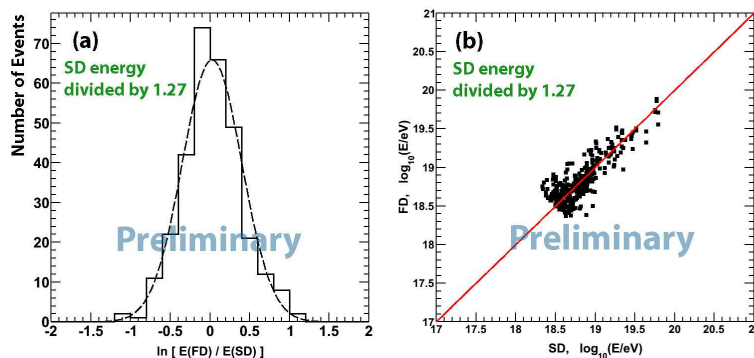


FIG. 9: (a) A histogram of the difference between FD and SD energies for hybrid events above 3×10^{18} eV. (b) A scatter-plot of the log FD energy vs. log SD energy for the same hybrid events.

from BR and LR, not shown here, are also consistent with those of the SD, and MD.

V. COMPOSITION AND ANISOTROPY

Since 2009, there has been a discrepancy in the X_{max} -based composition results between the AUGER and HiRes collaborations. AUGER claims to see a trend toward heavier composition at above 10^{19} eV [11], whereas HiRes results are consistent with a predominantly proton composition [12]. Figure 11 shows the first TA composition result based on X_{max} from stereo events. In Figure 11(a), the distribution of X_{max} for TA stereo events is compared to those of iron and proton events simulated with CORSIKA using the QGSJET-II hadronic model. It is clear that in mean value and in width of the distribution, the TA results are consistent with a predominantly protonic composition.

Figure 11(b) shows the plot of mean X_{max} vs. log energy for the same stereo data set. The various curves show the predictions (folding in detector response and trigger selection) of CORSIKA simulations with different hadronic interaction models. The TA data, like that for HiRes, is again consistent with a predominately protonic composition, especially when compared to QGSJET models. Composition studies based on the width of the X_{max} distributions, and on the width of the shower profiles as well as those using hybrid events are nearing completion.

The anisotropy searches in TA are based primarily on the SD data. After the first three years of observations, the data is entirely consistent with isotropy. We did check the TA data against the claim made by the AUGER collaboration in the 2007 Science article [13], where 8 of 13 AUGER events above 5.7×10^{19} eV were seen to be within 3.1° of Active galactic nuclei in the Veron-Cetty catalog [14] with $z < 0.018$. For the northern sky, the

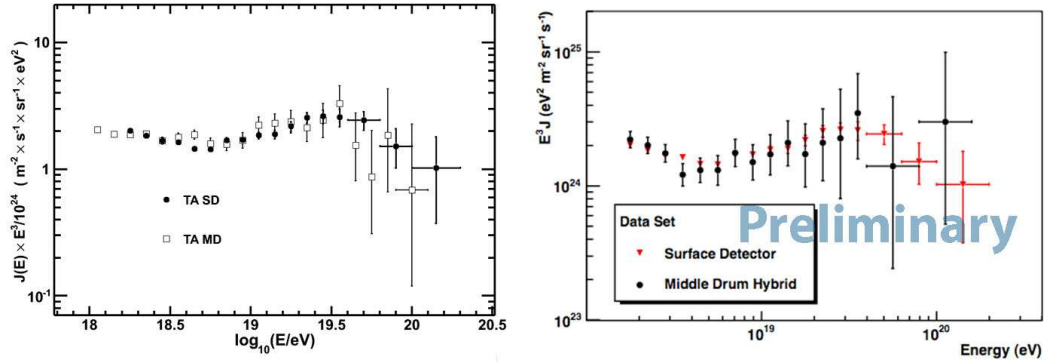


FIG. 10: (a) The TA surface detector spectrum with event energies scaled down by a factor of 1.27, overlaid with the monocular FD spectrum from Middle Drum. (b) The hybrid FD spectrum from Middle Drum overlaid with the energy-rescaled SD spectrum.

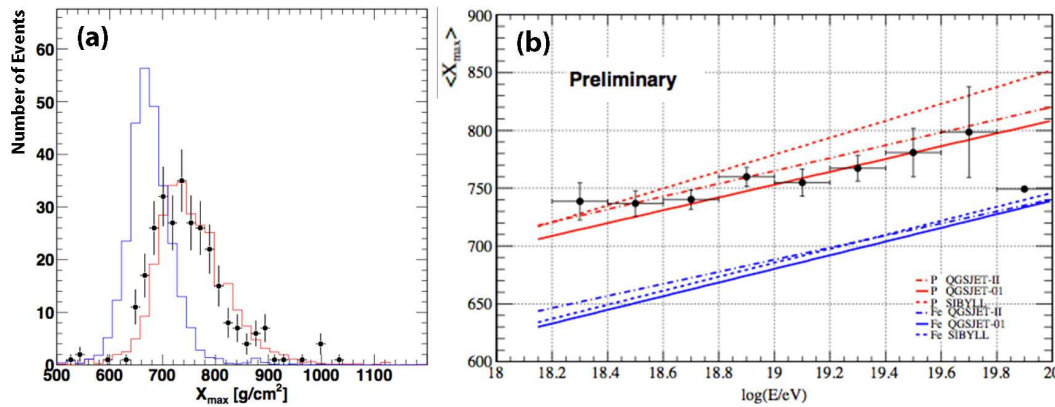


FIG. 11: (a) Distribution of shower maximum depth (X_{max}) of TA stereo data compared to CORSIKA simulation for proton and iron, based on the QGSJET-II hadronic interaction model. (b) Plot of mean X_{max} vs log energy for the same TA stereo data set. The accompanying curves show CORSIKA simulation results, including detector response and trigger selection effects for proton and iron with three different hadronic interaction models.

corresponding prediction for TA would have been 15 correlations out of 20 TA events seen above 5.7×10^{19} eV, whereas an isotropic distribution predicts five accidental correlations. Of these 20 events, eight were seen to be in coincidence with AGNs. This result is not a particularly significant departure ($p = 0.13$) from the null hypothesis. More TA data is needed for further anisotropy searches.

Acknowledgments

The Telescope Array experiment is supported by the Japan Society for the Promotion of Science through Grants-in-Aid for Scientific Research on Specially Promoted Research (21000002) “Extreme Phenomena in the Universe Explored by Highest Energy Cosmic Rays”, and the Inter-University Research Program of the Institute for Cosmic Ray Research; by the U.S. National Science Foundation awards PHY-0307098, PHY-0601915, PHY-0703893, PHY-0758342, and PHY-0848320 (Utah) and PHY-0649681 (Rutgers); by the National Research Foundation of Korea (2006-0050031, 2007-0056005, 2007-0093860, 2010-0011378, 2010-0028071, R32-10130); by the Russian Academy of Sciences, RFBR grants 10-02-01406a and 11-02-01528a (INR), IISN project No. 4.4509.10 and Belgian Science Policy under IUAP VI/11 (ULB). The foundations of Dr. Ezekiel R. and Edna Wattis Dumke, Willard L. Eccles and the George S. and Dolores Dore Eccles all helped with generous donations. The State of Utah supported the project through its Economic Development Board, and the University of Utah through the Office of the Vice President for Research. The experimental site became available through the cooperation of the Utah School and Institutional Trust Lands Administration (SITLA), U.S. Bureau of Land

Management and the U.S. Air Force. We also wish to thank the people and the officials of Millard County, Utah, for their steadfast and warm support. We gratefully acknowledge the contributions from the technical staffs of our home institutions and the University of Utah Center for High Performance Computing (CHPC).

-
- [1] Fukushima, M., Institute for Cosmic Ray Research Mid-term (2004 - 2009) Maintenance Plan Proposal Book "Cosmic Ray Telescope Project". 2002, Tokyo University. <http://www.telescopearray.org>
 - [2] N. Chiba *et al.*, Nucl. Instrum. Meth. **A311** (1992) 338; H. Ohoka, *et al.*, Nucl. Instrum. Meth. **A385** (1997) 268.
 - [3] T. Abu-Zayyad *et al.*, Proc. 26th ICRC, 4, 349 (1999); J. H. Boyer *et al.*, Nucl. Instr. Meth. **A482**, 457 (2002).
 - [4] R. M. Baltrusaitis *et al.*, Nucl Instrum. Meth. **A20**, 410 (1985).
 - [5] J. Linsely, J. Phys. G: Nucl. Phys., **12**, 51-57, 1986; D. Ikeda *et al.* Astrophys. Space Sci. Trans., **7**, 257263, (2011).
 - [6] S. Yoshida, N. Hayashida, K. Honda *et al.* J. Phys. G: Nucl. Phys., **20**, 651664, (1994).
 - [7] T. Gaisser and A. M. Hillas, Proc. 15th ICRC **8**, p. 353, (1977).
 - [8] K. Greisen, Phys. Rev. Lett. **16**, 48 (1968); T. Zatsepin and V. A. Kuzmin, Pis'ma Zh. Eksp. Teor. Fiz., **4**, 114 (1966).
 - [9] R. U. Abbasi *et al.* Phys. Rev. Lett. **92**, 151101 (2008).
 - [10] M. Takeda *et al.*, Astropart. Phys. **19**, 447 (2003).
 - [11] J. Abraham *et al.*, Phys. Rev. Lett. **104** 091101 (2010).
 - [12] R. U. Abbasi *et al.*, Phys. Rev. Lett. **104** 161101 (2010).
 - [13] The Auger Collaboration, Science, 318 p. 938, (2007).
 - [14] M.-P. Cetty and P. Veron, Astronomy and Astrophysics, **455**(2), p. 773, (2006).